Conf-930519--6

DETAILED SOLUTION TO A COMPLEX KINEMATICS CHAIN MANIPULATOR*

CONF-930519--6

DE93 004619

S. March-Leuba, J. F. Jansen, R. L. Kress, and S. M. Babcock
Robotics & Process Systems Division
Oak Ridge National Laboratory
Oak Ridge, Tennessee 37831-6304

To be presented at the
1993 IEEE International Conference on
Robotics and Automation
Atlanta, Georgia
May 2–7, 1993

*Research sponsored by the Office of Technology Development, U.S. Department of Energy, and the U.S. Army Human Engineering Laboratory, performed at Oak Ridge National Laboratory, managed by Martin Marietta Energy Systems, Inc., under contract DE-AC05-84OR21400.

DETAILED SOLUTION TO A COMPLEX KINEMATICS CHAIN MANIPULATOR*

S. March-Leuba, J. F. Jansen, R. L. Kress, and S. M. Babcock
Robotics and Process Systems Division
Oak Ridge National Laboratory
Oak Ridge, Tennessee 37831-6304

ABSTRACT

This paper presents a relatively simple method based on planar geometry to analyze the inverse kinematics for closed kinematics chain (CKC) mechanisms. Although the general problem and method of approach are well defined, the study of the inverse kinematics of a closed-chain mechanism is a very complicated one. The current methodology allows closed-form solutions to be found, if a solution exists, for the displacements and velocities of all manipulator joints. Critical design parameters can be identified and optimized by using symbolic models. This paper will focus on planar closed-chain structures extended with a rotational base. However, with open and CKC mechanisms combined in different planes, the extension to the case is straightforward. Further, real-time algorithms are developed that can be handled by existing microprocessor technology.

To clarify the methodology, the Soldier Robot Interface Project (SRIP) manipulator is analyzed, and a graphic simulation is presented as a verification of the results. This manipulator has 17 links, 24 one-degree-of-freedom (DOF) joints, and 7 CKC loops working in a plane and a rotational base, which determine its 3 DOFs. The SRIP manipulator allows a decoupled linear motion along the vertical or horizontal directions using only one of its linear actuators. The symbolic solution for the inverse kinematics allows optimization to be performed to further decouple the Cartesian motions by changing link lengths of the manipulator. The conclusion achieved by the optimization is that only two link lengths need to be changed to tune the manipulator for a perfect decoupling at each area of the workspace.

1. INTRODUCTION

In closed kinematics chain (CKC) manipulators, the moments and forces that move the links are typically transmitted through four-bar, five-bar, or higher planar-linkage mechanisms. These mechanisms are closed-chain structures having planar motion, used to supply rigidity and high end-effector force and to reduce dynamic and static loads due to the weight of motors by placing them closer to the base of the manipulator. For a serial link manipulator, a closed-form solution of the inverse kinematics is difficult, and most current 6-degree-of-freedom (DOF) serial-link manipulators are based on having the last three axes intersecting at a common point [Pieper, 68][1] because a closed-form solution is guaranteed to exist. However, with a CKC manipulator, the closed-form solution of the inverse kinematics is significantly more difficult. The link's spatial relationships can be described by holonomic constraint equations [Luh and Zheng, 85][2]. For each CKC loop a passive joint is selected and virtually cut, obtaining two holonomic constraint equations. Like the serial case, these equations are highly nonlinear. If this method is applied to the 7 closed-chain loops of the Soldier Robot Interface Project (SRIP) manipulator, then 14 independent nonlinear equations will be generated that are to be solved simultaneously giving 64 different joint solutions if joint limits and other physical considerations are ignored. Therefore, the Holonomic Constraints method was not suitable for practical application to the SRIP manipulator.

The ideal method to solve the inverse kinematics of manipulators that contain CKC loops should:

1. provide a closed-form solution for the joint displacements and speeds for both direct and inverse kinematics; and
2. present an efficient way to choose the correct solution because CKC robots always have several solutions, depending on the number of joints, links, and CKC loops.

The new method presented in this paper satisfies all of the above conditions. Most, if not all, CKC robots work in a plane only. This plane may be extended to a three-dimensional space by using a rotatory base and a 2- or 3-DOF hand. The general algorithm is presented with a direct application to the SRIP mamipulator after each of the following steps;

1. link connection description and reduction of the robot to its CKC plane,
2. finding the closed chain vector equations,
3. solving the inverse kinematics and joint speeds,
4. obtaining a closed-form for the inverse Jacobian of the CKC mechanism and extending it to the three-dimensional manipulator with a rotational base.

* Research sponsored by the Office of Technology Development, U.S. Department of Energy, and the U.S. Army Human Engineering Laboratory, performed at Oak Ridge National Laboratory, managed by Martin Marietta Energy Systems, Inc., under contract DE-AC05-84OR21400.

The graphic simulation for the CKC SRIP manipulator was implemented to verify the results of this paper.

2. SOLVING THE CKC MANIPULATOR

The algorithm presented in this paper has been applied to the SRIP manipulator. This device has 17 links, 24 one-DOF joints, and seven CKC loops working in a plane and a rotational base which determine its 3 DOF. This complicated manipulator allows a special movement of its end-effector. The CKC planar mechanism has only two linear actuators and one-dimensional movement in the vertical or the horizontal, achieved by moving only one of the motors. The base rotates the manipulator to reach an arbitrary point in 3-Dimensional space. (see Fig. 1.)

The number of DOFs in a CKC mechanism can be readily determined by Grübler's formula [Hunt, 78][3];

$$n = 3L - 2N_1 - N_2, \qquad (1)$$

n = Number of degrees of freedom,
L = Number of links, not including the fixed Base,
N_1 = Number of single degree-of-freedom joints,
N_2 = Number of two degree-of-freedom joints.

Therefore, the SRIP manipulator has:

$$\text{Number of DOF} = 3 \times 17 - 2 \times 24 - 0 = 3. \qquad (2)$$

2.1. Link Connection Description

This section discusses each component of the complete manipulator separately on the rotational base and the CKC mechanism. CKC robots are based on four-bar, five-bar, and higher planar-linkage mechanisms. If a linkage mechanism is not planar, then it can be projected into multiple planes and solved in a manner similar to the planar case. Because they are typical, the planar CKC will be the only case examined in detail in this paper; however, with open and closed kinematic chain mechanisms combined in different planes, the extension to the case is straightforward.

To describe the location of each link relative to its neighbors, we define a frame attached to each link. The link frames are named by number according to the link to which they are attached. That is, frame {i} is attached rigidly to link i, as in Craig's notation [Craig, 86][4]. As shown in Fig. 2, three different frames give the relationship between the components of the manipulator: base frame {B}, manipulator plane frame {M}, and end-effector frame {E}.

Thus, assuming that point ${}^{B}P = [x, y, z]^T$ written with respect to the base frame {B} is known, it is possible to obtain ${}^{M}P = [x_m, y_m]^T$ written with respect to the robot plane frame {M} and the angle θ_1, that must rotate the base.

$$\theta_1 = \text{Atan2}(y, x), \qquad (3a)$$

$$x_m = \sqrt{x^2 + y^2}, \qquad (3b)$$

$$y_m = z. \qquad (3c)$$

This transformation reduces the kinematic problem to the CKC manipulator plane, which simplifies the solution. All frames referred to links that belong to the CKC are attached with their Z axes perpendicular to the plane of the robot, defined by X_M and Y_M, simplifying all the transformation matrices between these frames.

The reduction of the manipulator to a plane allowed us to create a graphic simulation, that verified the results of this paper. Fig. 3 shows a wire-frame simulation of the SRIP manipulator in which all the links are included; the two linear actuators are represented by small squares attached to their links.

Once the three- to two-dimensional transformation has been accomplished, the next step is to number all the links and joints. Because all the links are in the same plane, each link can be represented as a two-dimensional vector. These vectors have the length of the link (r_i's) and the angle of the joint with the same number (θ_i's). Note that angles θ_i are absolute and measured from axis X_M, allowing us to take absolute instead of partial derivatives with respect to time later in this paper. These two-dimensional vectors can be written in complex form with respect to the X_M and Y_M axes by using Euler's formula as follows:

$$\bar{r}_n = r_n e^{i\theta_n} = r_n \cos\theta_n + i\, r_n \sin\theta_n. \qquad (4)$$

Some links may have more than two joints. For each extra joint, an extra vector is given until all the joints of all the links can be represented as an addition of planar vectors. As shown in Fig. 4 and 5:

(a) Links 2 through 7 and 12 through 16 are represented by vectors of constant lengths, $\bar{r}_6$
(b) Links 8 and 9 are represented by one variable length vector because of prismatic joints with respect to links 6 and 7 respectively.
(c) Links 1, 10, 11, and 17 are represented by more than one vector. As an example, link 10 is determined by three vectors because of its four joints.

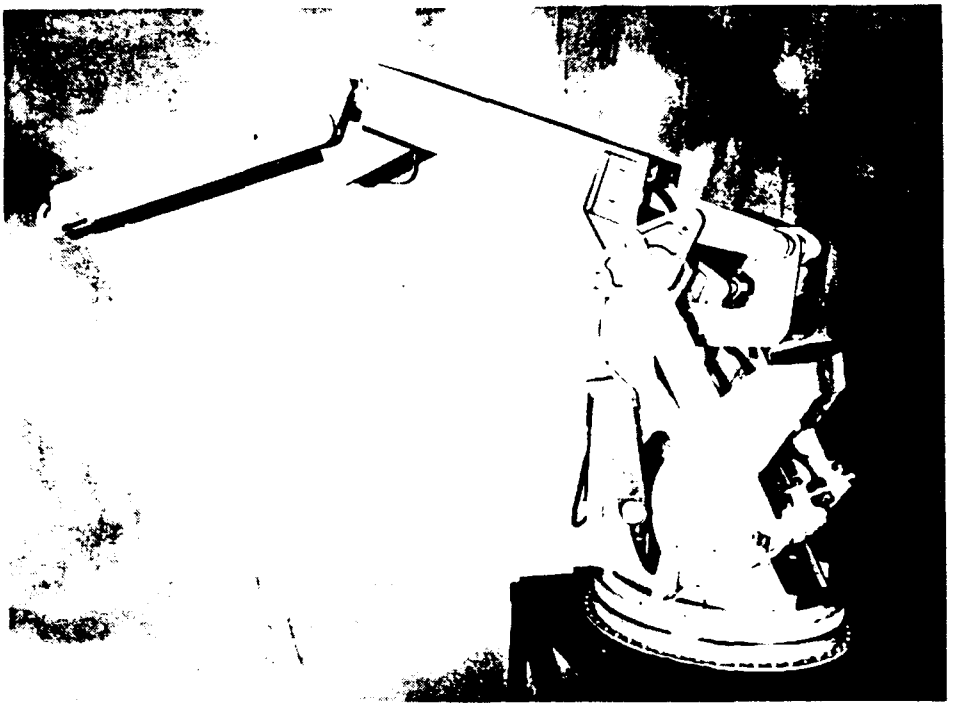

Fig. 1. Soldier Robot Interface Project manipulator (ORNL-Photo 5086-89).

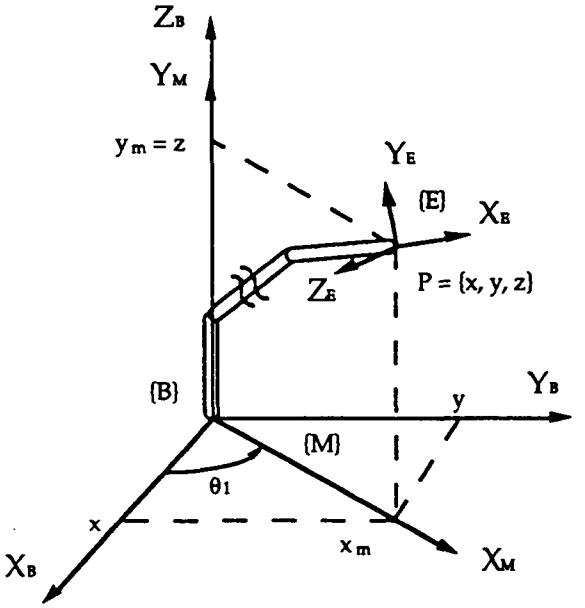

Fig. 2. Schematic diagram of a closed kinematic chain robot with its three frames.

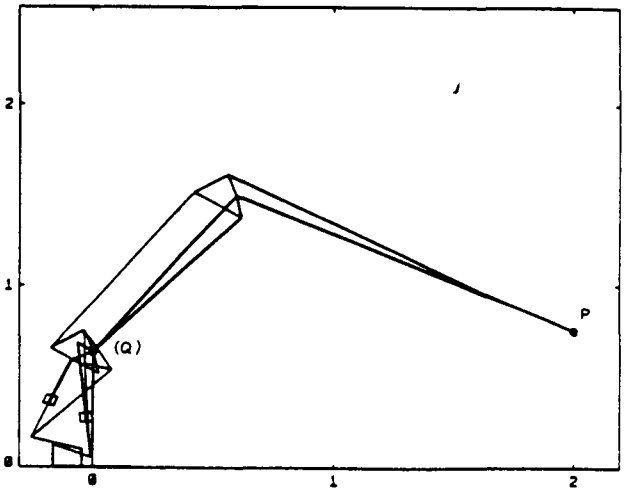

Fig. 3. Graphic simulation for the Soldier Robot Interface Project manipulator (dimensions are in meters).

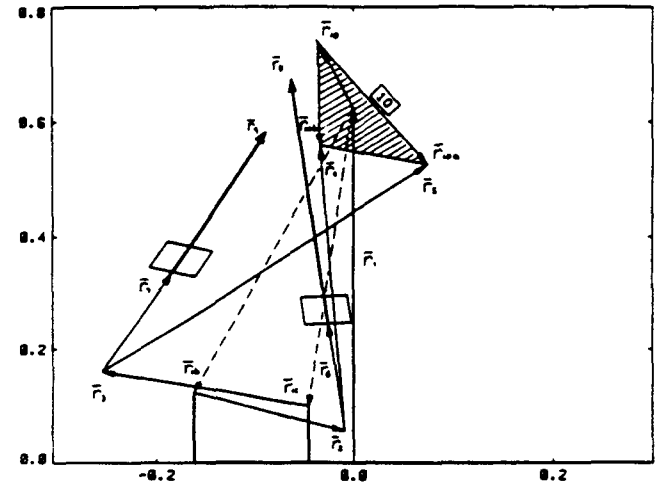

Figure 4. Soldier Robot Interface Project manipulator links 1 through 10 (dimensions in meters).

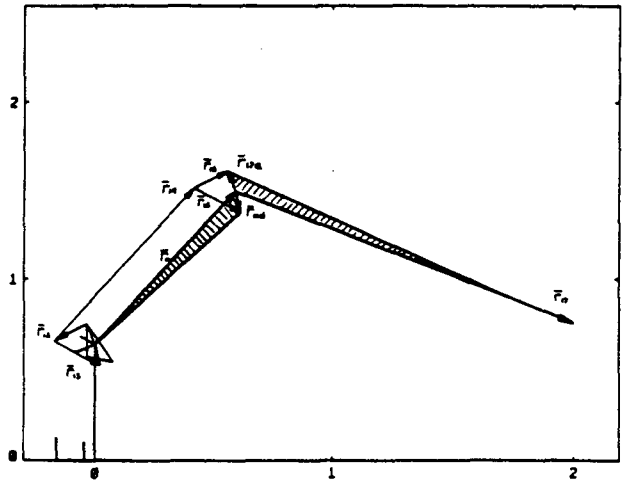

Fig. 5a. Soldier Robot Interface Project manipulator links 11 trough 17.

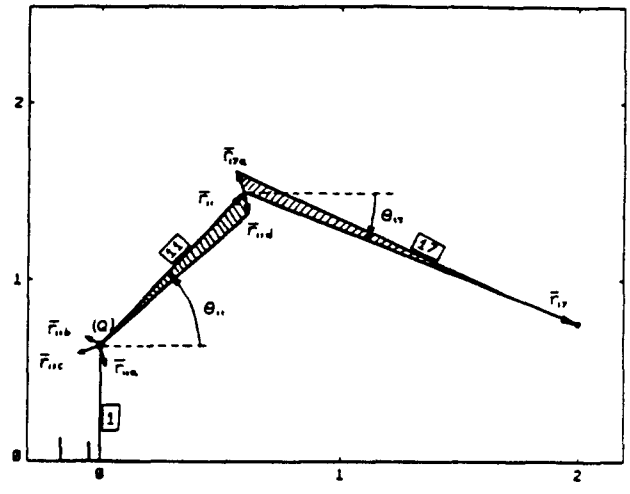

Fig. 5b. Soldier Robot Interface Project virtual manipulator.

2.2. Solving The Serial Virtual Manipulator

To solve the CKC planar mechanism, a reduced serial model must first be found. In a minimum number of links in the CKC mechanism, select the shortest way from the manipulator base to its end. Usually, a virtual open-chain robot exists with a 2-link arm; let us name it the virtual manipulator. As shown in Fig. 5, the shortest way through the SRIP manipulator is by using links 1, 11, and 17, which constitute its virtual serial manipulator. Now the CKC device has been separated into a virtual manipulator plus several virtual open-chains with origin and end points belonging to the virtual manipulator.

To solve for the displacement and speed of the joints that belong to the virtual manipulator, any known method for open-chain robots can be used [Craig, 86; Pieper, 68; Yoshikawa, 90]. Because this is a simple 2-DOF planar case, let us present a straightforward closed-form solution that will be used in obtaining not only the inverse kinematics solution for the virtual manipulator, but also for the rest of the SRIP manipulator joint values cases found in the SRIP manipulator CKC loops. Figures 6a and 6b present two possible cases found in the SRIP manipulator.

A closed-chain vector equation can be written for each of these two cases which locates vectors with unknown terms on the left-hand side while leaving on the right side all the known vectors:

$$r_a\, e^{i\theta_a} + r_b\, e^{i\theta_b} = r_s\, e^{i\theta_s}, \quad (5a)$$

$$(r_a + r_b)\, e^{i\theta_a} = r_s\, e^{i\theta_s}, \quad (5b)$$

where the unknown terms in Eq. (5a) are θ_a and θ_b, and those in Eq. (5b) are r_b and θ_a.

Fig. 6a presents the two possible solutions, elbow up or down, for the inverse kinematics of a planar 2-link rotational-joint manipulator of which link lengths are fixed. An inverse kinematic solution can be obtained by using an algebraic method similar to the ones presented in [Craig, 86] or [Yoshikawa, 90] but modified to handle multiple solutions for both angles, independently of the links location on the X-Y plane of Fig. 6a.

With the vector r_s, defined by point (x, y), and the length of the links known, the solution to the angles of the two links in Fig. 6a is found to be

$$\theta_a = \text{Atan2}(k\,x + k_a\,y, -k\,y + k_a\,x), \quad (6a)$$

$$\theta_b = \text{Atan2}(-k\,x + k_b\,y, k\,y + k_b\,x), \quad (6b)$$

$$r_s = \sqrt{x^2 + y^2}, \quad (6c)$$

$$k_b = \frac{r_b^2 - r_a^2 + r_s^2}{2\,r_s}, \quad (6d)$$

$$k_a = r_s - k_b, \quad (6e)$$

$$k = \pm\sqrt{r_b^2 - k_b^2}. \quad (6f)$$

Note that solution is not possible for the cases in which (1) $r_s = 0$; (2) $r_s > r_a + r_b$; or (3) $r_s < r_a - r_b$. The positive or negative square root in the formula for k above gives two possible solutions for angles θ_a and θ_b: (a) If $k > 0$, then $\theta_a - \theta_b > 0$: left side (elbow up), solid lines in Fig. 6a; (b) If $k < 0$, then $\theta_a - \theta_b < 0$: right side (elbow down), dashed lines in Fig. 6a.

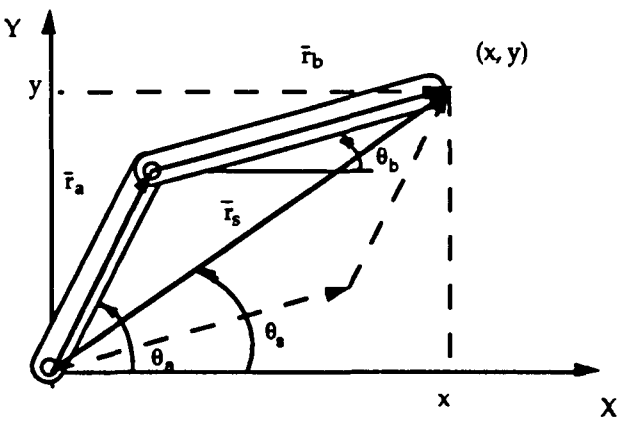

Fig. 6a. Planar 2-link rotational-joint manipulator.

Note that elbow up or down is usually referred to in the literature with respect to the gravity axis. Instead, in this paper, elbow up refers to elbow on the left side of the vector addition r_s, and elbow down means on the right side. When multiple solutions exist, some criteria are needed. This method provides a way of choosing by simple graphical iteration. As an example, in the SRIP manipulator, some specific configurations were needed to keep the weaker links of the CKC linkages in tension to prevent structural damage.

Fig. 6b presents a planar 2-link rotational-prismatic-joint manipulator. Because the vector r_s, defined by point (x, y), is known, the solutions to the unknowns (angle and length) are found to be

$$\theta_a = \text{Atan2}(y, x), \quad (7a)$$

$$r_b = \sqrt{x^2 + y^2} - r_a. \quad (7b)$$

For the virtual serial manipulator the closed chain vector equation, see Eq. 5 and Fig. 6, can be written for links 11 and 17 as follows:

$$r_{11}\, e^{i\theta_{11}} + r_{17}\, e^{i\theta_{17}} = x_m + i\,(y_m - r_1). \quad (8)$$

Showing their absolute angles solution to be

$$\theta_{11} = \text{Atan2}(k\,x_m + k_a(y_m - r_1), -k(y_m - r_1) + k_a\,x_m), \quad (9a)$$

$$\theta_{17} = \text{Atan2}(-k\,x_m + k_b(y_m - r_1), k(y_m - r_1) + k_b\,x_m), \quad (9b)$$

$$r_s = \sqrt{x_m^2 + (y_m - r_1)^2}, \quad (9c)$$

$$k_b = \frac{r_{17}^2 - r_{11}^2 + r_s^2}{2\,r_s}, \quad (9d)$$

$$k_a = r_s - k_b, \quad (9e)$$

$$k = +\sqrt{r_b^2 - k_b^2}. \quad (9f)$$

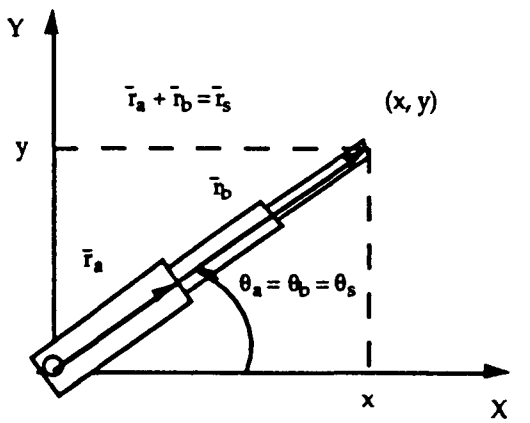

Fig. 6b. Planar rotational-prismatic joint manipulator.

Note that k was chosen to be positive, giving an elbow-up configuration for the SRIP virtual manipulator. This configuration is necessary to keep link 14 working on tension, as it was designed to be, when the manipulator is supporting a payload.

Once θ_{11} and θ_{17} have been calculated, then θ_{11a}, θ_{11b}, θ_{11c}, θ_{11d}, and θ_{17a} are also known because the vectors associated with these angles are attached rigidly to r_{11} and r_{17}.

2.3. Inverse Kinematics

The vectors that belong to the virtual manipulator, corresponding to links 1, 11, and 17, are known. Now, look for another set of unknown joined vectors r_a and r_b of constant lengths from which the initial point of the first and the final point of the second are known because they belong to the virtual manipulator. Or, in the case of prismatic joints, look for a single vector whose length and angle are unknown and its base and end points are known.

The general idea is to solve for the vectors that constitute the CKC in an iterative chain. Once the virtual manipulator is known, then find vectors attached to it and solve for them. Next, find vectors attached to these two and to the virtual manipulator and solve for them. The chain will lead to solving for the whole CKC system.

For every step in which another closed chain is found, a closed-chain vector equation [see Eq. (5)] can be written. For the SRIP manipulator, Eq. (10) can be written. Of the eight equations in Eqs. (10a) through (10h), one corresponds, to the virtual manipulator and the rest to the seven CKC loops that constitute the SRIP manipulator. Note that the terms on the right-hand side of each equation are known; therefore, each equation is cast into the form of Eq. (5a) or Eq. (5b). Each of these equations in complex form lead to two independent equations, one along the real axis and another along the complex axis.

Equations (8) and (9) describe an example solving Eq. (10a) for the absolute angles θ_{11} and θ_{17}. The method presented in Eqs. (6) and (7), can solve all the variables of the CKC system: θ_2, θ_3, θ_4, θ_5, θ_6, θ_7, R_8, R_9, θ_{10} (θ_{10a}, θ_{10b}), θ_{11} (θ_{11a}, θ_{11b}, θ_{11c}, θ_{11d}), θ_{12}, θ_{13}, θ_{14}, θ_{15}, θ_{16}, and θ_{17} (θ_{17a}).

Some of the vectors in Eq. (10), have a negative sign which is needed to create the closed-chain vector equations. To directly apply the solution presented by Eq. (6) it is easier to use only positive vectors on the left-hand side. To make the necessary transformation, note that in complex form

$$-r_a\, e^{i\theta_a} = r_a\, e^{i(\theta_a \pm \pi)}, \tag{11}$$

which is used next to solve for θ_{15} and θ_{16}, using Eqs. 6, 7, 10b, and 11:

$$\theta 16 = \text{Atan2}(k_1 x_1 + k_{1a} y_1, -k_1 y_1 + k_{1a} x_1) \pm \pi, \tag{12a}$$
$$\theta 15 = \text{Atan2}(-k_1 x_1 + k_{1b} y_1, k_1 y_1 + k_{1b} x_1), \tag{12b}$$

$$x_1 = -r_{17a}\cos\theta_{17a} + r_{11d}\cos\theta_{11d}, \tag{12c}$$
$$y_1 = -r_{17a}\sin\theta_{17a} + r_{11d}\sin\theta_{11d}, \tag{12d}$$
$$r_{1s} = \sqrt{x_1^2 + y_1^2}, \tag{12e}$$
$$k_{1b} = \frac{r_{15}^2 - r_{16}^2 + r_{1s}^2}{2 r_{1s}}, \tag{12f}$$
$$k_{1a} = r_{1s} - k_{1b}, \tag{12g}$$
$$k_1 = -\sqrt{r_{16}^2 - k_{1b}^2}. \tag{12h}$$

Note that k_1 has been chosen to be negative because from Fig. 5, it can be seen that vectors $-r_{16} + r_{15}$ are on

$$r_{11}\, e^{i\theta_{11}} + r_{17}\, e^{i\theta_{17}} = x_m + i(y_m - r_1), \tag{10a}$$
$$-r_{16}\, e^{i\theta_{16}} + r_{15}\, e^{i\theta_{15}} = -r_{17a}\, e^{i\theta_{17a}} + r_{11d}\, e^{i\theta_{11d}}, \tag{10b}$$

$$-r_{13}\, e^{i\theta_{13}} + r_{14}\, e^{i\theta_{14}} = -r_{11a}\, e^{i\theta_{11a}} + r_{11}\, e^{i\theta_{11}} + r_{11d}\, e^{i\theta_{11d}} - r_{15}\, e^{i\theta_{15}}, \tag{10c}$$
$$r_{10}\, e^{i\theta_{10}} + r_{12}\, e^{i\theta_{12}} = r_{11a}\, e^{i\theta_{11a}} - r_{13}\, e^{i\theta_{13}}, \tag{10d}$$
$$r_2\, e^{i\theta_2} + r_4\, e^{i\theta_4} = -r_{1b}\, e^{i\theta_{1b}} + r_{10}\, e^{i\theta_{10}} + r_{10b}\, e^{i\theta_{10b}}, \tag{10e}$$
$$r_3\, e^{i\theta_3} + r_5\, e^{i\theta_5} = -r_{1c}\, e^{i\theta_{1c}} + r_{10}\, e^{i\theta_{10}} + r_{10a}\, e^{i\theta_{10a}}, \tag{10f}$$
$$(r_6 + R_8)\, e^{i\theta_6} = -r_2\, e^{i\theta_2} - r_{1b}\, e^{i\theta_{1b}} + r_{11b}\, e^{i\theta_{11b}}, \tag{10g}$$
$$(r_7 + R_9)\, e^{i\theta_7} = -r_3\, e^{i\theta_3} - r_{1c}\, e^{i\theta_{1c}} + r_{11c}\, e^{i\theta_{11c}}. \tag{10h}$$

the right side or elbow down of the vector $-r_{17} + r_{11d}$. By the same method, solutions can be found for all the variables of the CKC. The positive or negative k_i's were chosen from Fig. 4 and 5 to be for (a) 11a $k > 0$, (b) 11b $k_1 < 0$, (c) 11c $k_2 > 0$, (d) 11d $k_3 < 0$, (e) 11e $k_4 < 0$, and (f) 11f $k_5 > 0$.

Equations (10g) and (10h) are easy to solve by applying Eq. (7). As an example, let us solve for R_8 and θ_6 from Eq. (10g):

$$\theta_6 = \text{Atan2}\,(y_g, x_g)\,. \tag{13a}$$

$$R_8 = \sqrt{x_g^2 + y_g^2} - r_6\,, \tag{13b}$$

$$x_g = -\,r_2 \cos\theta_2 - r_{1b} \cos\theta_{1b} + r_{11b} \cos\theta_{11b}\,, \tag{13c}$$

$$y_g = -\,r_2 \sin\theta_2 - r_{1b} \sin\theta_{1b} + r_{11b} \sin\theta_{11b}\,. \tag{13d}$$

In the same way solved for R_8, it can be solved for R_9 to find both SRIP manipulator linear motor movements. All the variables of the CKC robot have been found from its end-point position $P = [x, y, z]^T$ and its geometrical parameters. Therefore, the inverse kinematics for the CKC manipulator has been calculated.

2.4. Joint Speeds

To calculate the joint speeds of the links belonging to the CKC manipulator, take derivatives with respect to time of the closed-chain vector equations [see Eq. (10)]. The derivative with respect to time of a vector whose angle is absolute, measured from the X_M axis to itself, can be written in complex form as

$$\frac{d}{dt}\left[r_a\, e^{i\theta_a}\right] = \dot{r}_a\, e^{i\theta_a} + i\,\dot{\theta}_a\, r_a\, e^{i\theta_a}\,, \tag{14}$$

where $\dot{r}_a = 0$ if the link is rotational and of fixed length. Also, because absolute angles are used $\dot{\theta}_{10} = \dot{\theta}_{10a} = \dot{\theta}_{10b}$, $\dot{\theta}_{11} = \dot{\theta}_{11a} = \dot{\theta}_{11b} = \dot{\theta}_{11c} = \dot{\theta}_{11d}$, and $\dot{\theta}_{17} = \dot{\theta}_{17a}$.

As an example, let us solve first for the speeds of the SRIP virtual manipulator [Eq. (10a)] and then for links 15 and 16 [Eq. (10b)]. Finally, we will solve for $\dot{R}_8$, from Eq. (10g), to find the speed of one of the linear actuators of the SRIP manipulator.

Taking derivatives with respect to time of Eq. (10a),

$$i\,\dot{\theta}_{11}\, r_{11}\, e^{i\theta q_{11}} + i\,\dot{\theta}_{17}\, r_{17}\, e^{i\theta_{17}} = \dot{x}_m + i\,\dot{y}_m\,, \tag{15}$$

which can be separated into two independent equations: the first in the real axis and the second in the complex axis,

$$-\,\dot{\theta}_{11}\, r_{11} \sin\theta_{11} - \dot{\theta}_{17}\, r_{17} \sin\theta_{17} = \dot{x}_m\,, \tag{16a}$$

$$\dot{\theta}_{11}\, r_{11} \cos\theta_{11} + \dot{\theta}_{17}\, r_{17} \cos\theta_{17} = \dot{y}_m\,. \tag{16b}$$

By using C_i for $\cos(\theta_i)$ and S_i for $\sin(\theta_i)$, Eqs. (16a) and (16b) can be written in matrix formulation and solved for the speed of angles θ_{11} and θ_{17} by inverting a 2 x 2 matrix

$$\begin{bmatrix} \dot{\theta}_{11} \\ \dot{\theta}_{17} \end{bmatrix} = \begin{bmatrix} A_{11} & A_{12} \\ A_{21} & A_{22} \end{bmatrix} \begin{bmatrix} \dot{x}_m \\ \dot{y}_m \end{bmatrix} = \mathbf{A} \begin{bmatrix} \dot{x}_m \\ \dot{y}_m \end{bmatrix}, \tag{17a}$$

$$\mathbf{A} = \frac{-1}{r_{11}\, r_{17}\, S_{11\text{-}17}} \begin{bmatrix} r_{17}\, C_{17} & r_{17}\, S_{17} \\ -\,r_{11}\, C_{11} & -\,r_{11}\, S_{11} \end{bmatrix}, \tag{17b}$$

being $S_{11\text{-}17} = \sin(\theta_{11} - \theta_{17})$. The speed of angle θ_1 of the SRIP manipulator rotational base can be obtained by taking derivatives with respect to time of Eq. (3a) [Yoshikawa, 90]. After further reduction

$$\dot{\theta}_1 = \frac{\dot{y}\,x - \dot{x}\,y}{x^2 + y^2} = \frac{\dot{y}\,x - \dot{x}\,y}{x_m^2}\,, \tag{18a}$$

$$\dot{x}_m = \frac{x\,\dot{x}_m + y\,\dot{y}_m}{x_m}\,, \qquad \dot{y}_m = \dot{z}\,. \tag{18b}$$

To solve for the speed of angles θ_{15} and θ_{16}, take derivatives with respect to time of Eq. (10b),

$$-\,i\,\dot{\theta}_{16}\, r_{16}\, e^{i\theta_{16}} + i\,\dot{\theta}_{15}\, r_{15}\, e^{i\theta_{15}} = -\,i\,\dot{\theta}_{17}\, r_{17a}\, e^{i\theta_{17a}} + i\,\dot{\theta}_{11}\, r_{11d}\, e^{i\theta_{11d}}\,. \tag{19}$$

Separating the resulting equation into the real and complex axes and writing them in matrix form,

$$\begin{bmatrix} r_{15}\, C_{15} & -r_{16}\, C_{16} \\ -r_{15}\, S_{15} & r_{16}\, S_{16} \end{bmatrix} \begin{bmatrix} \dot{\theta}_{15} \\ \dot{\theta}_{16} \end{bmatrix} = \begin{bmatrix} r_{11d}\, C_{11d} & -r_{17a}\, C_{17a} \\ -r_{11d}\, S_{11d} & r_{17a}\, S_{17a} \end{bmatrix} \begin{bmatrix} \dot{\theta}_{11} \\ \dot{\theta}_{17} \end{bmatrix}. \tag{20}$$

By premultiplying the equation by the inverse of the matrix on the left-hand side and reducing trigonometrically, it is found that

$$\begin{bmatrix} \dot{\theta}_{15} \\ \dot{\theta}_{16} \end{bmatrix} = \mathbf{B} \begin{bmatrix} \dot{\theta}_{11} \\ \dot{\theta}_{17} \end{bmatrix}, \tag{21a}$$

$$\mathbf{B} = \frac{\begin{bmatrix} r_{16}\, r_{11d}\, S_{11d\text{-}16} & r_{16}\, r_{17a}\, S_{16\text{-}17a} \\ r_{15}\, r_{11d}\, S_{11d\text{-}15} & r_{15}\, r_{17a}\, S_{15\text{-}17a} \end{bmatrix}}{-\,r_{15}\, r_{16}\, S_{16\text{-}15}}\,. \tag{21b}$$

To solve for the speeds of angle θ_6 and length R_8, one of the linear actuators, take derivatives with respect to time of Eq. (10g),

$$i\,\dot{\theta}_6\,(r_6 + R_8)\,e^{i\theta_6} + \dot{R}_8\,e^{i\theta_6} = -i\,\dot{\theta}_2\,r_2\,e^{i\theta_2} + i\,\dot{\theta}_{11}\,r_{11b}\,e^{i\theta_{11b}}. \quad (22)$$

Note that r_{1b}, like r_{1c}, is just a constant vector on the XM-YM plane. Separating the resulting equation into the real and complex axes, writing them in matrix form, and premultiplying the equation by the inverse of the matrix on the left-hand side as was done in Eq. (20), it is found that

$$\begin{bmatrix} \dot{\theta}_6 \\ \dot{R}_8 \end{bmatrix} = \mathbf{O} \begin{bmatrix} \dot{\theta}_2 \\ \dot{\theta}_{11} \end{bmatrix}, \quad (23a)$$

$$\mathbf{O} = \frac{\begin{bmatrix} r_2\,C_{6\text{-}2} & -r_{11b}\,C_{11b\text{-}6} \\ (r_6+R_8)r_2\,S_{6\text{-}2} & (r_6+R_8)r_{11b}\,S_{11b\text{-}6} \end{bmatrix}}{-(r_6+R_8)}. \quad (23b)$$

Any of the joint variables can be solved similarly. Finding the following matrix relations:

$$\begin{bmatrix} \dot{\theta}_{11} \\ \dot{\theta}_{17} \end{bmatrix} = \mathbf{A}\begin{bmatrix} \dot{x}_m \\ \dot{y}_m \end{bmatrix}, \quad \begin{bmatrix} \dot{\theta}_{15} \\ \dot{\theta}_{16} \end{bmatrix} = \mathbf{B}\begin{bmatrix} \dot{\theta}_{11} \\ \dot{\theta}_{17} \end{bmatrix},$$
$$\begin{bmatrix} \dot{\theta}_{13} \\ \dot{\theta}_{14} \end{bmatrix} = \mathbf{D}\begin{bmatrix} \dot{\theta}_{15} \\ \dot{\theta}_{11} \end{bmatrix}, \quad \begin{bmatrix} \dot{\theta}_{10} \\ \dot{\theta}_{12} \end{bmatrix} = \mathbf{F}\begin{bmatrix} \dot{\theta}_{13} \\ \dot{\theta}_{11} \end{bmatrix}, \quad (24)$$
$$\begin{bmatrix} \dot{\theta}_2 \\ \dot{\theta}_4 \end{bmatrix} = \mathbf{H}\begin{bmatrix} \dot{\theta}_{10} \\ \dot{\theta}_{10} \end{bmatrix}, \quad \begin{bmatrix} \dot{\theta}_3 \\ \dot{\theta}_5 \end{bmatrix} = \mathbf{L}\begin{bmatrix} \dot{\theta}_{10} \\ \dot{\theta}_{10} \end{bmatrix},$$
$$\begin{bmatrix} \dot{\theta}_6 \\ \dot{R}_8 \end{bmatrix} = \mathbf{O}\begin{bmatrix} \dot{\theta}_2 \\ \dot{\theta}_{11} \end{bmatrix}, \quad \begin{bmatrix} \dot{\theta}_7 \\ \dot{R}_9 \end{bmatrix} = \mathbf{P}\begin{bmatrix} \dot{\theta}_3 \\ \dot{\theta}_{11} \end{bmatrix}.$$

The inverse kinematics and the joint velocities have been calculated. By further extending the application of this methodology for real time computation, a closed form for the inverse Jacobian can be found.

2.5. The Inverse Jacobian

The Jacobian of a robot is the matrix relation between the speed of its motors and the Cartesian speeds of its end effector. After we have obtained the speed of all the joints of the CKC robot and knowing the ones of the end-effector, the inverse of the Jacobian is obtained in this section.

To compute the inverse Jacobian, first the inverse sub-Jacobian of the CKC planar manipulator is calculated with respect to the Cartesian movement on the plane of the robot. From Eq. (24), the following relations are obtained:

$$\dot{R}_8 = O_{21}\,\dot{\theta}_2 + O_{22}\,\dot{\theta}_{11}, \quad (25a)$$
$$\dot{R}_9 = P_{21}\,\dot{\theta}_3 + P_{22}\,\dot{\theta}_{11}, \quad (25b)$$
$$\dot{\theta}_2 = (H_{11} + H_{12})\,\dot{\theta}_{10}, \quad (25c)$$
$$\dot{\theta}_3 = (L_{11} + L_{12})\,\dot{\theta}_{10}, \quad (25d)$$
$$\dot{\theta}_{10} = F_{11}\,\dot{\theta}_{13} + F_{12}\,\dot{\theta}_{11}, \quad (25e)$$
$$\dot{\theta}_{13} = D_{11}\,\dot{\theta}_{15} + D_{12}\,\dot{\theta}_{11}, \quad (25f)$$
$$\dot{\theta}_{15} = B_{11}\,\dot{\theta}_{11} + B_{12}\,\dot{\theta}_{17}. \quad (25g)$$

After substituting, reducing, and collecting terms, we can write the following expression for the two linear motor speeds:

$$\dot{R}_8 = T_1\,\dot{\theta}_{11} + T_2\,\dot{\theta}_{17}, \quad (26a)$$
$$\dot{R}_9 = T_3\,\dot{\theta}_{11} + T_4\,\dot{\theta}_{17}, \quad (26b)$$

$$T_1 = O_{22} + O_{21}(H_{11}+H_{12})(F_{12}+F_{11}\,D_{12}+F_{11}\,D_{11}\,B_{11}), \quad (26c)$$
$$T_2 = O_{21}(H_{11}+H_{12})(F_{11}\,D_{11}\,B_{12}), \quad (26d)$$
$$T_3 = P_{22} + P_{21}(L_{11}+L_{12})(F_{12}+F_{11}\,D_{12}+F_{11}\,D_{11}\,B_{11}), \quad (26e)$$
$$T_4 = P_{21}\,(L_{11}+L_{12})(F_{11}\,D_{11}\,B_{12}). \quad (26f)$$

Finally, applying the following relation from Eq. (24)

$$\dot{\theta}_{11} = A_{11}\,\dot{x}_m + A_{12}\,\dot{y}_m, \quad (27a)$$
$$\dot{\theta}_{17} = A_{21}\,\dot{x}_m + A_{22}\,\dot{y}_m, \quad (27b)$$

we find the inverse sub-Jacobian for the planar CKC mechanism to be

$$\begin{bmatrix} \dot{R}_8 \\ \dot{R}_9 \end{bmatrix} = \begin{bmatrix} IJ_{p11} & IJ_{p12} \\ IJ_{p21} & IJ_{p22} \end{bmatrix}\begin{bmatrix} \dot{x}_m \\ \dot{y}_m \end{bmatrix}, \quad (28a)$$

$$IJ_{p11} = T_1\,A_{11} + T_2\,A_{21},$$
$$IJ_{p12} = T_1\,A_{12} + T_2\,A_{22},$$
$$IJ_{p21} = T_3\,A_{11} + T_4\,A_{21}, \quad (28b)$$
$$IJ_{p22} = T_3\,A_{12} + T_4\,A_{22}.$$

By using Eq. (18), we can write the inverse Jacobian for the SRIP manipulator as

$$\begin{bmatrix} \dot{R}_8 \\ \dot{R}_9 \\ \dot{\theta}_1 \end{bmatrix} = \begin{bmatrix} Ij_{p11}\frac{x}{x_m} & Ij_{p11}\frac{y}{x_m} & Ij_{p12} \\ Ij_{p21}\frac{x}{x_m} & Ij_{p21}\frac{y}{x_m} & Ij_{p22} \\ \frac{-y}{x_m^2} & \frac{x}{x_m^2} & 0 \end{bmatrix} \begin{bmatrix} \dot{x} \\ \dot{y} \\ \dot{z} \end{bmatrix} \quad (29)$$

To prove the correctness of the solution for the Jacobian, it was compared with numerical methods of perturbing the inverse kinematics solution. Instead of derivatives with respect to time, an incremental approximation for the speed of each motor was taken:

$$\Delta R_8 = Ij_{p11}\frac{x}{x_m}\Delta x + Ij_{p11}\frac{y}{x_m}\Delta y + Ij_{p12}\Delta z \; . \quad (30)$$

Different points in the space with the robot were tested, and the results were accurately to 4 decimal places.

3. WORKSPACE DEFINED BY KINEMATIC AND MECHANICAL CONSTRAINTS

In this section, the workspace for the SRIP manipulator is studied and plotted. Geometrical constraints due to link lengths, link tension constraints to prevent structural damage, and joint range constraints are considered.

Because of its rotational base, the workspace of the SRIP manipulator is a volume of revolution. Therefore, it is necessary to study its workspace only in the plane that the first joint defines.

The lengths of the links that constitute the SRIP virtual manipulator [r_1 = 66.04 cm (26 in.), r_{11} = 109.22 cm (43 in.), and r_{17} = 134.62 cm (53 in.)] already constrain the workspace to a circle of radius $r_{11} + r_{17}$ = 243.84 cm (96 in.) around the point P($x_m = 0$, $y_m = r_1$) on the plane of the CKC planar mechanism.

The larger four-bar linkage of the SRIP manipulator includes links 11, 13, 14, and 15. The thin, weaker link (14) was designed to work on tension but not on compression. For link 14 to work on tension, the positive square root in the formula for k [see Eq. (9f)] must be used. In addition, to keep the same constraint, when θ_{11} is larger than 90°, then θ_{17} cannot be allowed to exceed 90°.

Because the SRIP manipulator has only 3-DOFs only three independent joint ranges are necessary to constrain its workspace. In particular, the angular range constraints for the SRIP virtual manipulator (see Fig. 5) are those that best define its workspace. The joint limits for the SRIP virtual manipulator and rotational base were measured to be approximately: $-180° \le \theta_1 \le 180°$, $-90° \le \theta_{11} \le 150°$, and $-150° \le \theta_{17} - \theta_{11} \le 0°$.

For the given constraints, the workspace for the SRIP manipulator is identified by the patterned area in Fig. 7. The inverse kinematics, workspace, and plotting functions were implemented in Mathematica [Wolfram, 88].

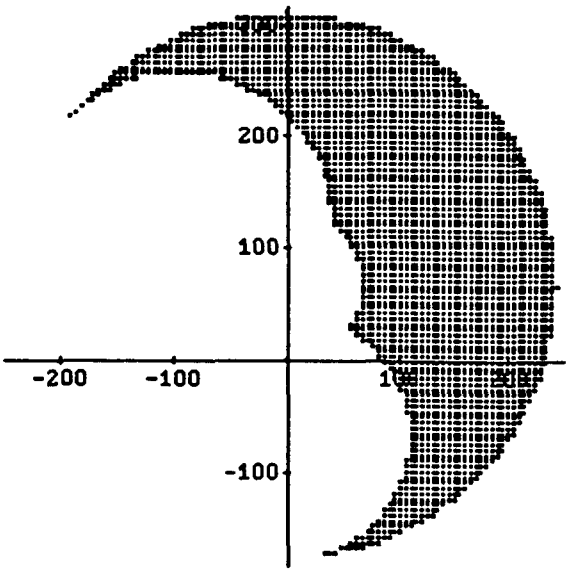

Fig. 7. Workspace of the SRIP manipulator (dimensions are in centimeters).

The three-dimensional workspace for the SRIP manipulator is obtained by rotating the patterned area in Fig. 7 around the vertical axis.

4. OPTIMIZATION OF THE SRIP ARM MOVEMENT

The SRIP manipulator allows a special movement of its end effector: the CKC planar manipulator's sub-Jacobian [see Eq. (28)], relating its two linear actuators with the Cartesian end effector movement is almost diagonal for a specific area of the workspace. This allows an almost decoupled linear motion along the horizontal or vertical directions using only one of its linear actuators. The symbolic solution for the inverse kinematics allows optimization to be performed to further decouple the Cartesian motions by changing link lengths of the manipulator. The conclusion achieved by the optimization is that only two link lengths need to be changed to tune the manipulator for perfect decoupling at each area of the workspace.

From Eqs. (10) and (24), it can be concluded that matrices **H** and **O** are independent of r_3, and matrices **L** and **P** are independent of r_2. Further, Eq. (26) shows that

T_1 and T_2 are independent of r_3, and T_3 and T_4 are independent of r_2. This conclusion leads to the following:

$\dot{R}_8$ is dependent on r_2 but independent of r_3. (31a)

$\dot{R}_9$ is dependent on r_3 but independent of r_2. (31b)

Further, the effect of the linear actuator 8 (or 9) on the manipulator end point can be tuned by changing r_2 (or r_3) without interfering with the effect of the other actuator.

The idea is to create a close-to-perfect diagonal sub-Jacobian for the planar CKC mechanism by driving IJ_{p12} and IJ_{p21} [see Eq. (28)] to zero, changing the values for r_2 and r_3 respectively. Different values for r_2 and r_3 were found for different positions on the plane defined by axes X_M and Y_M. Figure 10 shows the element IJ_{p12} of the inverse Jacobian varying with the change in length (r_2) of link 2, while IJ_{p21} stays constant for a particular position in the space of the SRIP manipulator.

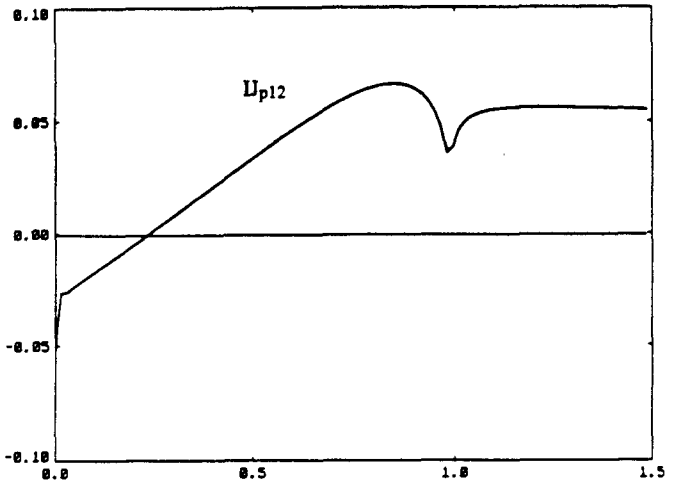

Fig. 10. IJ_{p12} as a function of r_2 (dimensions are in meters for r_2).

The lengths r_2 and r_3 that make IJ_{p12} and IJ_{p21} equal to zero will give a diagonal sub-Jacobian, tuning the SRIP manipulator for an area of the space close to where it is working. For different areas of the workspace, different values were found for the tune up.

5. CONCLUSION

A relatively simple method to solve the inverse kinematics for manipulators that contain closed-chain mechanisms is presented in this paper. Closed-form solution for angles and speeds of joints' displacements are obtained. Finding the Jacobian of the robot and its inverse is very useful. Also, a proof for angles and speeds is shown with the graphic simulation and the approximation for the Jacobian.

To verify the results of this paper a graphic simulation for the SRIP manipulator was used. This graphic simulation works in the inverse direction given joint solutions, draw the robot beginning from the base to the end point. Figures (3 through 5) plotted with this graphic simulation show the robot working in different positions and orientations.

The methodology presented in this paper was applied to solve the SRIP manipulator, which has 17 links, 24 one-DOF joints, and 7 CKC loops working in a plane and a rotational base that determine its 3-DOFs. Optimization of some link lengths for tuning the decoupling of the Cartesian movement produced by its actuators was accomplished by taking advantage of the closed-form solutions obtained. The method presented uses uncomplicated numerical methods, so it is well suited for real-time implementation.

ACKNOWLEDGMENTS

This research was supported in part by an appointment to the U.S. Department of Energy Postgraduate Research Program at the Oak Ridge National Laboratory administered by Oak Ridge Associated Universities. The authors thank the U.S. Army Human Engineering Laboratory, who sponsored the Small Business Innovative Research grant under which the arm was developed. We also acknowledge Odetics, Inc., the company that developed the SRIP manipulator.

REFERENCES

[Craig, 86] John J. Craig, Introduction to Robotics Mechanics and Control, Addison-Wesley Publishing Company, Reading, Mass., ISBN#0-201-10326-5, 1986.

[Hunt, 78] Hunt, K. H., Kinematic Geometry of Mechanisms, Oxford University Press, 1978.

[Luh and Zheng, 85] J. Y. S. Luh and Yuan-Fang Zheng, "Computation of Input Generalized Forces for Robots with Closed Kinematic Chain Mechanisms," IEEE Journal of Robotics and Automation, Vol. RA-1, No. 2, June 1985.

[Pieper, 68] D. Pieper, "The Kinematics of Manipulators Under Computer Control" Ph.D. thesis, Stanford University, Stanford, Calif., 1968.

[Wolfram, 88] S. Wolfram, Mathematica: A System for Doing Mathematics by Computer, Addison-Wesley Publishing Company, Scotts Valley, Calif, ISBN#0-201-51507-5, 1988.

[Yoshikawa, 90] T. Yoshikawa, Foundations of Robotics: Analysis and Control, MIT Press, ISBN# 0-262-24028-9, 1990.